REPORT DOCUMENTATION PAGE

Form Approved
OMB No. 0704-0188

1. AGENCY USE ONLY *(Leave blank)*	2. REPORT DATE	3. REPORT TYPE AND DATES COVERED
	May 28, 1998	10/1/93 - 9/30/97

4. TITLE AND SUBTITLE
New Theories for Erosion-Corrosion: ASSERT Supplement

5. FUNDING NUMBERS
N00014-93-I-1113

6. AUTHOR(S)
Mark E. Orazem

7. PERFORMING ORGANIZATION NAMES(S) AND ADDRESS(ES)
Department of Chemical Engineering
PO Box 116005
University of Florida
Gainesville, FL 32611-6005

8. PERFORMING ORGANIZATION REPORT NUMBER

9. SPONSORING / MONITORING AGENCY NAMES(S) AND ADDRESS(ES)
Department of the Navy
Office of Naval Research
Materials Division
Office of Chief of Naval Res., Arlington, VA 22217-5000

10. SPONSORING / MONITORING AGENCY REPORT NUMBER

11. SUPPLEMENTARY NOTES

a. DISTRIBUTION / AVAILABILITY STATEMENT
Unlimited

DISTRIBUTION STATEMENT A
Approved for public release;
Distribution Unlimited

19980604 039

13. ABSTRACT *(Maximum 200 words)*

The erosion-corrosion of copper and copper-nickel alloys in synthetic seawater was investigated using an impinging jet. Video microscopy, corrosion potential monitoring, and impedance spectroscopy were used to investigate the state of the system and the reactivity of the electrode surface. Shear-induced removal of salt films was observed and found to be associated with significant increases in surface reactivity. Direct shear-induced removal of oxide films, however, was not observed. Nevertheless, the protective oxide layer showed sensitivity in passively aerated seawater to large fluid velocities and to small perturbations in potential. The films were stable under all conditions tested in continuously aerated seawater. The present work supports the argument that localized corrosion of copper alloys is caused by galvanic coupling between different regions of a metal coupon. The potential difference driving the galvanic couple could originate from localized shear-induced removal of salt films as well as from non-uniformly distributed oxygen transport rates.

14. SUBJECT TERMS	15. NUMBER OF PAGES
erosion-corrosion, copper, copper-nickel alloys, impedance spectroscopy, impinging jet	23
	16. PRICE CODE

17. SECURITY CLASSIFICATION OF REPORT	18. SECURITY CLASSIFICATION OF THIS PAGE	19. SECURITY CLASSIFICATION OF ABSTRACT	20. LIMITATION OF ABSTRACT
unlimited	unlimited	unlimited	unlimited

TABLE OF CONTENTS

LIST OF TABLES

LIST OF FIGURES

SUMMARY OF RESULTS

The ASSERT supplement supported the dissertation research of Paul T. Wojcik. The objective of Paul's research was to investigate the corrosion of copper and copper-nickel alloys under high-shear flow of synthetic seawater. The principle accomplishments of Paul's research include:

Variable-Amplitude Galvanostatically Modulated Impedance Spectroscopy

An algorithm was developed described in which galvanostatic regulation of electrochemical impedance measurements was conducted with an amplitude of current perturbation adjusted at each frequency to yield a desired variation in potential. Measurements of three previous frequencies were used to estimate the value of the impedance at the target frequency. The algorithm was implemented using a graphically-based general interfacing software on a personal computer. Experimental results illustrated artifacts that can arise as a result of galvanostatic measurement with fixed current amplitude or as a result of potentiostatic measurements for systems with a changing corrosion potential. A demonstration is presented of the use of variable-amplitude galvanostatically modulated impedance spectroscopy to monitor the corrosion of copper in synthetic seawater. This approach provided a critical step in developing a method to monitor the natural evolution of a corroding system without changing the system behavior.

Preliminary Interpretation of Data

A methodology was developed to allow use of the measurement model approach to quantify differences in surface reactivity in the absence of specific process models.[1] The interpretation of the spectra presented here followed: a) identification of the frequency-dependent stochastic component of the error structure following the method presented by Agarwal *et al.*[2] This information was used to weight subsequent regressions; b) identification of the portion of the spectrum that is consistent with the Kramers-Kronig relations following the method presented by Agarwal *et al.*;[3,4] c) Regression of the measurement model to the part of the spectrum found to be consistent with the Kramers-Kronig relations. The regressed parameter values were used to extrapolate the zero frequency limit and Monte Carlo simulations were performed using the standard deviations of the regressed parameters to estimate the confidence interval for the extrapolation. The polarization impedance was obtained by subtracting the regressed solution resistance from the extrapolated zero frequency value. This approach allowed extraction of reactivity data in the absence of a specific model for the corrosion of copper in seawater.

Experimental Study of Shear-Induced Removal of Films

The erosion-corrosion of copper and copper-nickel alloys in synthetic seawater was investigated using an impinging jet. Video microscopy, corrosion potential monitoring, and impedance spectroscopy were used to investigate the state of the system and the reactivity of the electrode surface. Shear-induced removal of salt films was observed and found to be associated with significant increases in surface reactivity. Direct shear-induced removal of

oxide films, however, was not observed. Nevertheless, the protective oxide layer showed sensitivity in passively aerated seawater to large fluid velocities and to small perturbations in potential. The films were stable under all conditions tested in continuously aerated seawater. The present work supports the argument that localized corrosion of copper alloys is caused by galvanic coupling between different regions of a metal coupon. The potential difference driving the galvanic couple could originate from localized shear-induced removal of salt films as well as from non-uniformly distributed oxygen transport rates.

Resulting Publications and Presentations

Under support from this contract, Paul contributed to the following publications and presentations. Copies of the publications will be provided in the final report for the contract N00014-93-I-0056.

Refereed Publications

1. P. T. Wojcik, P. Agarwal, and M. E. Orazem, "A Method for Maintaining a Constant Potential Variation during Galvanostatic Regulation of Electrochemical Impedance Measurements," *Electrochimica Acta,* **41** (1996), 977-983.
2. P. T. Wojcik and M. E. Orazem, "Variable-Amplitude Galvanostatically-Modulated Impedance Spectroscopy as a Tool for Assessing Reactivity at the Corrosion Potential without Distorting the Temporal Evolution of the System," *Corrosion*, **54** (1998) 289-298.
3. M. E. Orazem, P. T. Wojcik, M. Durbha, I. Frateur, and L. H. García-Rubio, "Application of Measurement Models for Interpretation of Impedance Spectra for Corrosion," *Materials Science Forum,* in press.

Refereed Conference Proceedings

1. P. T. Wojcik and M. E. Orazem, "Variable-Amplitude Galvanostatically Modulated Impedance Spectroscopy as a Non-Invasive Tool for Assessing Reactivity at the Corrosion Potential," Paper #97-282, National Association of Corrosion Engineers, Houston, Texas, 1997.
2. P. T. Wojcik and M. E. Orazem, "Experimental Study of the Erosion-Corrosion of Copper and Copper-Nickel Alloys Using a Submerged Impinging Jet," Paper #97-435, National Association of Corrosion Engineers, Houston, Texas, 1997.
3. P. T. Wojcik, E. Charrière, and M. E. Orazem, "Experimental Study of the Erosion-Corrosion of Copper and Copper-Nickel Alloys at the Corrosion Potential and at Anodic Potentials," *Proceedings of the Tri-Service Conference on Corrosion,* November 17-21, 1997.

Manuscripts Submitted or in Preparation

1. P. T. Wojcik, E. Charrière, and M. E. Orazem, "Experimental Study of the Erosion-Corrosion of Copper and Copper-Nickel Alloys at the Corrosion Potential and at Anodic Potentials," submitted to *Corrosion.*

Presentations

1. P. T. Wojcik, P. Agarwal, and M. E. Orazem, "A Method for Maintaining a Constant Potential Variation during Galvanostatic Regulation of Electrochemical Impedance Measurements," presented at the Third International Symposium on Electrochemical Impedance Spectroscopy, Ysermonde, Belgium, May 7-12, 1995.
2. P. T. Wojcik, P. Agarwal, and M. E. Orazem, "Variable-Amplitude Galvanostatically Modulated Impedance Spectroscopy as a Non-Invasive Tool for Assessing Reactivity at the Corrosion Potential," presented at the 2nd Workshop on Quantitative Methods for Predicting Coating Performance, Annapolis, Maryland, November 1-3, 1995.
3. P. T. Wojcik and M. E. Orazem, "Evaluation of Corrosion under Controlled Flow by Variable-Amplitude Galvanostatically Modulated Impedance Spectroscopy and Video Microscopy," presented at the 190th Meeting of the Electrochemical Society, San Antonio, Texas, October 10, 1996.
4. P. T. Wojcik and M. E. Orazem, "Variable-Amplitude Galvanostatically Modulated Impedance Spectroscopy as a Non-Invasive Tool for Assessing Reactivity at the Corrosion Potential," paper 97-282 presented at Corrosion/97, New Orleans, Louisiana, March 9-14, 1997.
5. P. T. Wojcik and M. E. Orazem, "Experimental Study of the Erosion-Corrosion of Copper and Copper-Nickel Alloys Using a Submerged Impinging Jet," paper 97-435 presented at Corrosion/97, New Orleans, Louisiana, March 9-14, 1997.
6. M. E. Orazem, P. T. Wojcik, I. Frateur, and L. H. García-Rubio, "Application of Measurement Models for Interpretation of Impedance Spectra for Corrosion," (keynote lecture) presented at Electrochemical Methods for Corrosion Research, EMCR 97, Trento, Italy, August 25-29, 1997.
7. P. T. Wojcik, E. Charrière, and M. E. Orazem, "Experimental Study of the Erosion-Corrosion of Copper and Copper-Nickel Alloys at the Corrosion Potential and at Anodic Potentials," presented at the Tri-Service Conference on Corrosion, November 17-21, 1997.

Dissertation

1. Paul T. Wojcik, *The Electrochemical Behavior of Copper and Copper Nickel Alloys in Synthetic Seawater,* University of Florida, August, 1997.

INTRODUCTION

Copper and copper alloys are widely used in marine environments because they are resistant to corrosion in seawater. This resistance is associated with formation of protective layers on the metal surface. However, copper and its alloys are known to be susceptible to enhanced corrosion in seawater when there is sufficient relative motion between the metal and the fluid.[5-7] The flow-enhanced corrosion of copper alloys in seawater has been attributed to erosion-corrosion.[6]

In the absence of suspended particles, erosion-corrosion is associated with mechanical disruption or removal of protective layers by hydrodynamic shear.[6,8,9] Protective layers are assumed to be removed when the shear force is greater than the binding force between the film and the substrate. Direct observation of shear-induced removal of films has been reported for some systems. Giralt and Trass[10] showed that removal of solid naphthalene and trans-cinnamic acid by a submerged impinging jet of saturated solution is proportional to the wall shear stress above a critical or threshold value. Steele and Geankoplis[11] reported removal of material by an apparent shear erosion mechanism. Esteban *et al.*[12] used an impinging jet system to identify shear-induced removal of poorly adhered filming inhibitors on steel in chloride solutions. The removal of the inhibitor was associated with enhanced corrosion in regions of large hydrodynamic shear.

Efird reported critical values of shear stress for the erosion-corrosion of copper and some copper-based alloys in seawater (see Table 1).[6] His test apparatus consisted of a series of independent flow chambers with a rectangular cross section designed such that fresh seawater flowed parallel to the surface of the coupon. Flow establishment and disengagement regions were located up and downstream respectively to ensure a well-developed flow over the coupon. Coupons were removed and photographed after a thirty-day exposure. Accelerated corrosion was identified by the roughened appearance of corrosion products and of the metal surface after corrosion products were removed. A critical velocity for enhanced corrosion was identified which was correlated to shear stress. Onset of enhanced corrosion was consistently located at the leading edge of the coupon.

The experimental system used by Efird[6] was characterized by a uniform shear stress and a non-uniform mass transfer coefficient. While Efird[6] attributed observation of a critical velocity for enhanced corrosion to a shear-induced removal of protective films, it could also be explained by destabilization of the protective films by a differential mass-transfer mechanism. Melton *et al.* have attributed enhanced corrosion of copper alloys associated with large fluid velocities to a distribution of oxygen transport rates to the copper surface.[13] Macdonald *et al.* conducted a systematic study of the influence of oxygen on corrosion of copper alloys and concluded that the apparent erosion-corrosion was caused by formation of differential oxygen-transfer cells.[14-17] Nevertheless, the argument that shear-induced removal of protective films causes erosion-corrosion continues in the literature. Silverman[18] presented correlation between corrosion rates and shear stress, and Efird[19] has recently provided results of a comprehensive comparison of experimental techniques based on shear stress.

The studies of Macdonald, *et al.*[14-17] and Melton, *et al.*[13] used flow-by arrangements, such as that used by Efird,[6] for which shear stress was uniform and mass transfer was non-uniform. Such a system should be sensitive to galvanic couples caused by differential aeration but not to galvanic couples caused by non-uniform removal of surface films by hydrodynamic forces. The impinging jet geometry used by Diem and Orazem[20] is attractive for investigation of the role of hydrodynamic forces. The radial variation of shear stress makes removal of films by hydrodynamic shear visible and, under certain design constraints, mass transfer can be made uniform, thereby eliminating differential oxygenation cells. Using the impinging jet geometry, Diem and Orazem[21] did not observe shear-induced corrosion on copper in alkaline chloride electrolytes for values of hydrodynamic shear which were as much as 10 times the critical shear stress reported by Efird.[6] In the alkaline chloride solutions used, passivation was observed in less than 100 seconds. The work of Diem and Orazem[21] cannot be compared directly to that of Efird[6] because the electrolyte was significantly different in composition from the seawater used in Efird's experiment. Steady-state films on copper alloys in seawater are reported to require 30 days or more to develop.[22-25]

The objective of this work was to determine whether shear-induced removal of protective films for copper and copper-nickel alloys could be observed in systems for which mass transfer is uniform. The exposure time for the coupons was up to 33 days, and ASTM standard synthetic seawater was used as the electrolyte.

EXPERIMENTAL PROCEDURE

The hydrodynamics and the experimental design for the submerged axisymmetric impinging jet used in this study are presented in this section.

Hydrodynamics of the Impinging Jet

The flow pattern within the region of the electrode is well-defined.[26-30] This geometry can be made to give uniform mass transfer rates across a disk electrode within the stagnation region. The stagnation region is defined to be the region surrounding the stagnation point in which the axial velocity, given by

$$v_z = -2\sqrt{a\nu}\phi(\eta) \tag{1}$$

is independent of radial position, and the radial velocity is given by

$$v_r = ar\frac{d\phi(\eta)}{d\eta} \tag{2}$$

where a is the hydrodynamic constant which is a function only of geometry and fluid velocity, r and z are the radial and axial positions, respectively, ν is the kinematic viscosity, and ϕ is the stream function which is given in terms of dimensionless axial position $\eta = z\sqrt{a/\nu}$ as[30]

$$\phi(\eta) = 0.656\eta^2 - 0.16667\eta^3 + 3.6444\times10^{-3}\eta^6 - 3.9682\times10^{-4}\eta^7 \tag{3}$$

Esteban *et al.* used ring electrodes to find that the stagnation region extends to a radial distance roughly equal to the inside radius of the nozzle.[12]

Within the stagnation region, the surface shear stress τ_{rz} is given by

$$\tau_{rz} = -1.312r(\mu\rho)^{\frac{1}{2}}a^{\frac{3}{2}} \tag{4}$$

where μ and ρ are the viscosity and density of the fluid, respectively. The hydrodynamic constant is proportional to the jet velocity. It can be determined experimentally using ring or disk electrodes at the mass-transfer-limited condition.[12,21] The shear stress on the electrode surface is given in Figure 1 as a function of jet velocity for the range of velocities used in this work. The critical shear stress values reported by Efird[2] for copper (9.4 N/m^2) and 70/30 copper nickel (47.9 N/m^2) are provided for reference in Figure 1.

Experimental Design

Because the mass transfer rate is uniform, differential mass transfer cells are not established for an electrode that lies entirely within the stagnation region. The impinging jet system can therefore be used in the absence of suspended particles to isolate the influence of the hydrodynamic shear stress. If the removal of protective layers by hydrodynamic shear is the primary cause of erosion-corrosion and the shear stress outside a certain critical radius is large enough to cause that removal, then the metal outside the critical radius will corrode at a significantly higher rate than the metal inside the critical radius. Since shear stress is a function of both radial position and jet velocity, the critical radius corresponding to the critical shear stress would be a function of jet velocity for fixed geometry.[12]

A schematic representation of the experimental setup is presented in Figure 2. The experimental impinging jet cell used for this work was a modification of the cell design used by Diem and Orazem.[21] The cell was enclosed completely to eliminate entrainment of air. The system was capable of continuous operation at a maximum mean jet velocity of 6.75 m/s which yielded a shear stress of 195 N/m^2 at 80% of the radius of a 0.635 cm (0.25 inch) diameter electrode. This value is 20 times larger than the critical shear stress of 9.8 N/m^2 reported by Efird for copper.[6]

The system was configured with the jet positioned facing down. The top sides of the impinging jet cell were angled at 45° and 60° from vertical and an access port was centered in each side to allow in-situ observation of the working electrode. The port which supported the video microscope contained a sapphire window sealed with an o-ring and held in place by an aluminum retaining ring. The other access port housed a thermometer to monitor cell temperature which was compared with reservoir temperature. At high flow rates, viscous dissipation caused the temperature in the cell to differ from that in the reservoir. The temperature in the cell was controlled at a desired value by adjusting the set-point temperature in the cooling bath.

Three *in-situ* experimental techniques were incorporated in this work. The corrosion potential with reference to a saturated calomel reference electrode was monitored continuously throughout the course of an experiment. Variable-amplitude

galvanostatically-modulated (VAG) impedance spectroscopy was used at specified intervals to investigate the reactivity of the electrode surface.[31,32] The VAG technique allowed collection of impedance data without altering the natural evolution of the corrosion potential with time. Video microscopy complimented the two electrochemical techniques by providing a visual record of the state of the electrode surface. Digital images of the surface were used to detect velocity-enhanced phenomena which were manifested as rings or halos on the surface of the disk electrode.

The surface reactivity was quantified through use of the measurement model approach.[1-4,33-35] This quantification followed three steps:

1. The frequency-dependent error structure was identified following the method presented by Agarwal et al.[2]
2. The portion of the spectrum that is consistent with the Kramers-Kronig relations was identified following the method presented by Agarwal et al.[3,4] The error structure found in step 1 above was used to weight the regression. High-frequency data were found to be corrupted by instrumental artifacts. The low-frequency data were typically found to be consistent with the Kramers-Kronig relations except for data collected under conditions where the corrosion potential was changing rapidly.
3. The measurement model was regressed to the portion of the spectrum found in step 2 to be consistent with the Kramers-Kronig relations. The regressed parameter values were used to extrapolate to the zero frequency limit, and Monte Carlo simulations were performed using the standard deviations of the regressed parameters to estimate the confidence interval for the extrapolation. The polarization impedance was obtained by subtracting the regressed solution resistance from the extrapolated zero-frequency value.[1]

RESULTS

The experiments discussed here involved annealed electrodes made of 99.9% copper (CDA110) or a 70/30 copper/nickel alloy (CDA715). The electrolyte was ASTM-D-1141 synthetic seawater.

Copper in Passively-Aerated Electrolyte

In the experiments presented in this section, the electrolyte was aerated only by passive diffusion of air through the exposed air-electrolyte interface in the reservoir. The pH was measured to be 8.05, and the oxygen content of the electrolyte was 6 ppm. In the subsequent section, results are presented for continuously-aerated electrolytes, for which the air used for aerating the electrolyte was scrubbed to remove CO_2. Continuous aeration had no effect on the pH of the electrolyte, which remained at 8.2. The oxygen content of the continuously and passively-aerated electrolytes was 7 and 6 ppm, respectively.

Potentiostatic Experiments

The utility of the experimental setup for detecting shear-induced removal of films can be seen in the results of experiments conducted for 99.9% copper electrode in flowing (0.1 m/s) aerated synthetic seawater at anodic potentials. The current-time traces resulting from potentiostatic experiments are given in Figure 3 for values of 100, 200, and 400 mV (SCE). These potentials corresponded to regions of the polarization curve that were influenced by formation of salt films which, as seen in Figure 3, to decrease the current observed. The 200 mV (SCE) trace showed a decrease in the current followed by a sharp increase that was evident at roughly 300 seconds. Successive video images were collected at a rate of 2/second for this experiment. The dashed lines in Figure 3 are the times corresponding to the video images given in Figure 4 of the coupon during the 200 mV(SCE) experiment. At short times (33 and 61 seconds), growth of salt films reduced the magnitude of the current. Following the current distribution on a disk electrode below the limiting current,[36] salt films formed first as a ring on the periphery of a copper disk electrode and then grew inward. During the early stage of dissolution (0 to 160 seconds), the video images showed three waves corresponding to formation of salt films. At 160 seconds, the beginning stage of the mechanical removal of a salt film layer was evident at the periphery of the electrode. (see Figure 4). This removal was coincident with a slight increase in current evident in Figure 3. At 341 seconds, more of the film has been removed, and, at still longer times, the film was removed completely and a new salt film was precipitated. The removal of the salt film caused a 30 percent increase in the observed current. The removal process initiated at the periphery of the electrode where the shear stress is largest, and mechanical removal of chunks of the film was evident in the video. This experiment, conducted at anodic potentials, was used to establish that hydrodynamic forces can remove salt films and that removal of salt films is associated with an increase in corrosion current.

Galvanostatic Experiments at the Corrosion Potential.

The working electrode was 99.9% copper immersed in ASTM-D-1141 synthetic seawater. The corrosion potential is presented in Figure 5 as a function of time for a period of 33 days. The initial corrosion potential behavior of all the copper and copper/nickel alloys studied for this work was similar in the sense that the corrosion potential, immediately after submersion, increased rapidly during the first few hours.[37] As the corrosion potential became more positive, the rate of change slowed until a constant value was reached. The difference between the initial value and the constant value was as much as 70 mV. Electrohydrodynamic impedance measurements conducted under similar conditions showed that the electrochemical behavior of copper in synthetic seawater became insensitive to convective diffusion within 24 hours; thus, the electrochemical behavior of the copper was controlled by surface films after the first day of immersion.

The jet velocity for the first seven days was controlled at 1 m/s. A pseudo-steady-state value of -283 mV(SCE) for the corrosion potential was reached after approximately 48 hours, and this value fluctuated by only 2 mV over the next five days. Impedance spectra collected during this same seven day period showed an initial decrease in the

impedance followed by an increase to a pseudo-steady-state value. Following the seventh day, the solution was kept quiescent for 16 days after which a series of impedance scans was conducted to investigate corresponding changes in the electrode reactivity. Impedance scans taken before and after the 16 day quiescent period revealed an increase in the polarization impedance during period of time the solution was stagnant. Video images of the copper surface revealed the presence of a thick film.

After 556.6 hours, a large cathodic potential on the order of -1.3 V(SCE) was applied to the system for approximately 2 minutes resulting in the evolution of hydrogen from the electrode surface and removal of copper oxides. The impedance values after the potential excursion were reduced by a factor of 10 as compared to the impedance scans prior to the upset. A noticeable change in the appearance of the electrode surface was evident, and the presence of hydrogen bubbles on the surface was observed in the video images. The decrease in the impedance observed after the potential disturbance is consistent with removal of a protective film. This hypothesis is supported by the digital images that showed that portions of a surface film were removed, leaving bare copper visible around the periphery of the electrode.

Approximately 25 minutes after the potential disturbance, flow was resumed. Air that had accumulated in the lines was removed, after which the jet velocity was adjusted to 1 m/s. Data collection resumed 25 minutes after flow was started, and the resulting corrosion potentials are presented in Figure 6. The corrosion potential returned to the value before the potential disturbance after a period of 120 hours and remained constant for several days. A small adjustment of pH by addition of NaOH had no discernible effect on the corrosion potential. The corrosion potential changed abruptly, however, following an increase in jet velocities of 1.0 to 6.75 m/s. The values for the shear stress corresponding to these velocities at a radial position of $r/r_0 = 0.8$ are 14.5 and 195 N/m^2, respectively.

Impedance data collected during this leg of the experiment are presented in Figure 7. The impedance increased steadily after the potential disturbance, showing a decrease in reactivity as the protective films became reestablished. The value for the impedance approached a constant value after an additional 150 hours. The influence of pH modification from 8.05 to 8.24 on the impedance response was not discernible when plotted in impedance plane format, however, the influence of a change in jet velocity from 1.0 to 6.75 m/s on the impedance of the electrode is easily seen in Figure 7.

The polarization impedance corresponding to Figure 7 is shown in Figure 8 as a function of time. The polarization impedance and the associated confidence intervals given in Figure 8 were obtained by the measurement model concept developed in this group as part of the infrastructure for the erosion-corrosion experiments.[33-Error! Bookmark not defined.] The polarization impedance increased with time. The impedance response was found to be sensitive to the small adjustment of pH and also showed a large increase in the reactivity of the surface following the increase in jet velocity.

The video micrographs shown in Figure 9 can give insight on the evolution of the electrode surface. The copper electrode at t=0, immediately after submersion in solution, showed polishing marks left by the 0.05 μm alumina powder used in the final stage of wet

polishing. The presence of a uniform film at t=169 hours is consistent with electrohydrodynamic impedance spectroscopy measurements that showed that the electrochemical properties of the copper were governed by surface films after 24 hours of immersion. A similar uniform film was observed at t=671 hours after the system recovered from the potential excursion. After the increase in jet velocity, which resulted in a large reduction in the polarization impedance, a uniform film was still evident (t=814 hours). The apparently increased sharpness as compared to the image at t=671 hours is attributed to removal of a salt film, exposing the granular structure below. No ring-shaped features were evident in the micrographs.

The sensitivity reported here to velocity was reproducible for passively aerated electrolytes. In early experiments for copper, the polarization resistance stabilized within a period of 4 days. Increase of jet velocities to values corresponding to 14 to 16 times Efird's reported critical shear stress for copper changed the polarization resistance. For the same system, a sinusoidal potential perturbation of only 50 mV caused a large and irreversible decrease in the polarization resistance.[31] These results confirm that protective films can become unstable under even a small potential perturbation.

Copper and 70/30 Copper/Nickel in Continuously-Aerated Electrolyte at the Corrosion Potential

The abrupt increase in reactivity with increased jet velocity shown in Figure 8 was reproducible for passively-aerated electrolytes, but was not observed for copper in continuously-aerated electrolyte. The corrosion potential transients shown in Figure 10 are typical of the results obtained in aerated ASTM-D-1141 synthetic seawater. Effects of velocity on corrosion potential were not seen. The extrapolated polarization impedance values given in Figure 11 showed that the surface reactivity stabilized after a period of 10 days and that increases in jet velocity from 1 m/s to 2 m/s, from 2 m/s to 4 m/s, and from 4 m/s to 6.2 m/s had no discernible effect. Ex-situ analysis by XPS of the electrodes after immersion in continuously-aerated electrolyte revealed the presence of Mg and Fe salts that were not present on electrodes after immersion in passively-aerated electrolyte. These results, and observation of a small decrease in pH in the passively-aerated case, are consistent with the hypothesis that the nature of surface films formed had changed due to passive incorporation of CO_2 through the air-electrolyte interface in the reservoir.

The corrosion potential of the 70/30 copper nickel alloy in continuously aerated ASTM-D-1141 synthetic seawater reached a steady value within 5 days, though the measurement had considerably more scatter than observed for the copper system. The extrapolated polarization impedance values showed that surface reactivity stabilized after a period of 10 days, and that increases in jet velocity from 2 m/s to 6 m/s had no discernible effect.

CONCLUSIONS

Fully-developed oxide layers were observed in earlier work to be sensitive to small amplitude (50 mV) perturbations in potential.[31] Flow conditions resulting in a variation of potential across a copper surface can therefore disrupt protective oxide layers, not by direct

mechanical removal, but by inducing electrochemical instability. Salt films resulting from an applied anodic potential were observed to be removed by shear forces, and removal of such films increased the reactivity of copper. This removal of salt films on parts of the electrode and not on others could contribute to a potential gradient that would destabilize oxide layers. Oxygenation cells are another source of potential gradients which could form when using a channel flow cell such as used by Efird.[6].

The coupling of the VAG impedance algorithm and the extrapolation of impedance spectra developed for this work provides a powerful tool for assessing changes in the reactivity of an electrode. By setting the current to be equal to zero, galvanostatic modulation allowed the system to be held at the open-circuit condition, and the variable-amplitude technique ensured that the potential swing the system experienced was sufficiently small to ensure a linear response. The latter is particularly important because, in earlier work, a potential perturbation of 50 mV was sufficient to disrupt the passive films formed on copper in passively-aerated ASTM-D-1141 synthetic seawater.[31] The VAG impedance technique used in this work did not appear to affect the naturally occurring transients in the system associated with growth of surface films. The extrapolation technique developed here was intended to make maximum use of the available measurements by providing a convenient measure of reactivity. This was especially important in developing an assessment of the data presented in Figure 7 where the rapidly changing conditions made some low frequency data inconsistent with the Kramers-Kronig relations.

The films formed on copper in passively-aerated synthetic seawater appeared to be less stable than those formed in highly-aerated synthetic seawater. Such films were found here to be sensitive to changes in jet velocity. In earlier work, these films were found to be sensitive as well to changes in sinusoidal potential swings.[31] This result is consistent with the numerical simulations of Moghissi which predicted that the oxide layers on copper would be sensitive to pH and, in the pH ranges typical of seawater, could be unstable to small perturbations of potential.[38]

Shear-induced removal of oxide layers was not observed in the present work. However, the observations that salt-films on copper could be removed by hydrodynamic forces and that the removal of such films causes a significant increase in current may explain why the controversy over the role of hydrodynamic forces in erosion-corrosion continues in the literature. The present work supports the argument that localized corrosion of copper alloys is caused by galvanic coupling between different regions of a metal coupon.[13-17] The present work demonstrates that the potential difference driving the galvanic couple could originate from localized shear-induced removal of salt films as well as from non-uniformly distributed oxygen transport rates.

REFERENCES

[1] M. E. Orazem, P. T. Wojcik, M. Durbha, I. Frateur, and L. H. García-Rubio, "Application of Measurement Models for Interpretation of Impedance Spectra for Corrosion," *Materials Science Forum,* in press.

[2] P. Agarwal, O. D. Crisalle, M. E. Orazem, and L. H. García-Rubio, *Journal of the Electrochemical Society,* **142** (1995), 4149-4158.

[3] P. Agarwal, M. E. Orazem, and L. H. García-Rubio, *Journal of the Electrochemical Society,* **142** (1995), 4159-4168.

[4] P. Agarwal, M. E. Orazem, and L. H. García-Rubio, *Electrochemical Impedance: Analysis and Interpretation,* J. Scully, D. Silverman, M. Kendig, Editors, American Society for Testing and Materials, Philadelphia, 1993, 115-139.

[5] F.L. LaQue, Marine Corrosion: Causes and Prevention, John Wiley and Sons, N.Y. (1975).

[6] K.D. Efird, *Corrosion,* **33** (1977), 3.

[7] R.J.K. Wood, S.P. Hutton, and D.J. Schiffrin, *Corrosion Science,* **30** (1990), 1177.

[8] H.R. Copson, *Corrosion,* **16** (1960), 86t.

[9] D. C. Silverman, *Corrosion,* **40** (1984), 220-226.

[10] F. Giralt, and O. Trass, *Canadian Journal of Chemical Engineering,* **53** (1975), 505.

[11] L. R. Steele, and C. J. Geankoplis, *AIChE Journal,* **5** (1959), 178.

[12] J. M. Esteban, G. Hickey, and M. E. Orazem, *Corrosion,* **46** (1990), 896.

[13] D. G. Melton, R. M. McGowan, and M. W. Joseph, Paper 276, Corrosion/86, NACE International, 1986.

[14] D. D. Macdonald, B. C. Syrett, and S. S. Wing, *Corrosion,* **34** (1978), 289.

[15] D. D. Macdonald, B. C. Syrett, and S. S. Wing, *Corrosion,* **35** (1979), 367.

[16] B. C. Syrett, D. D. Macdonald, and S. S. Wing, *Corrosion,* **35** (1979), 367. 409

[17] B. C. Syrett and D. D. Macdonald, *Corrosion,* **35** (1979), 505.

[18] D. C. Silverman, *Corrosion,* **40** (1984), 220-226.

[19] K. D. Efird, E. J. Wright, J. A. Boros, and T. G. Hailey, *Corrosion,* **49** (1993) 992.

[20] C. B. Diem and M. E. Orazem, *Corrosion,* **50** (1994), 290.

[21] C. B. Diem and M. E. Orazem, *Corrosion,* **50** (1994), 290.

[22] H. P. Hack and J. P. Gudas, "Inhibition of Sulfide-Induced Corrosion by Clean Seawater Pre-exposure," Report DTNSRDC/SME-79-85, David Taylor Naval Ship Research and Development Center, 1979.

[23] J. R. Scully, H. P. Hack, and D. G. Tipton, *Corrosion,* **42** (1986), 462.

[24] H. P. Hack and J. R. Scully, *Corrosion,* **45** (1986), 79.

[25] H.P. Hack and H.W. Pickering, *Journal of the Electrochemical Society,* **138** (1991), 690.

[26] M. T. Scholtz, and O. Trass, *AIChE Journal,* **16** (1970), 82.

[27] M. T. Scholtz, and O. Trass, *AIChE Journal,* **16** (1970), 90.

[28] F. Giralt, C.-J. Chia, and O. Trass, *Industrial and Engineering Chemistry, Fundamentals,* **16** (1977), 21.

[29] C.-J. Chia, F. Giralt, and O. Trass, *Industrial and Engineering Chemistry, Fundamentals,* **16** (1977), 28.

[30] D.-T. Chin, and C.-H. Tsang, *Journal of the Electrochemical Society,* **125** (1978), 1461.

[31] P.T. Wojcik, P. Agarwal, and M. E. Orazem, *Electrochimica Acta,* **41** (1996), 977-983.

[32] P. T. Wojcik and M. E. Orazem, *Corrosion*, **54** (1998) 289-298.

[33] P. Agarwal, M. E. Orazem, and L. H. García-Rubio, *Journal of the Electrochemical Society,* **139** (1992), 1917-1927.

[34] P. Agarwal, O. C. Moghissi, M. E. Orazem, and L. H. García-Rubio, *Corrosion,* **49** (1993), 278-289.

[35] M. E. Orazem, P. Agarwal, and L. H. García-Rubio, *Materials Science Forum,* **192-194** (1995), 563-572.

[36] M. E. Orazem and M. G. Miller, *Journal of the Electrochemical Society,* **134** (1987), 392-399.

[37] P. Agarwal, O. C. Moghissi, M. E. Orazem, and L. H. García-Rubio, *Corrosion,* **49** (1993), 278-289.

[38] O. C. Moghissi, *The Electrochemical Behavior of Copper in Chloride Solutions,* PhD dissertation, University of Florida, May, 1993.

Table 1. Critical velocity and shear stress for copper-based alloys in seawater as reported by Efird.[6]

Alloy / main components	Critical Velocity, m/s	Temperature, °C	Critical Shear, Stress N/m^2
CA 122 copper	1.3	17	9.6
CA 687 copper /zinc	2.2	12	19.2
CA 706 90/10 copper/nickel	4.5	27	43.1
CA 715 70/30 copper/nickel	4.1	12	47.9
CA 722 copper/nickel/chromium	12.0	27	296.9

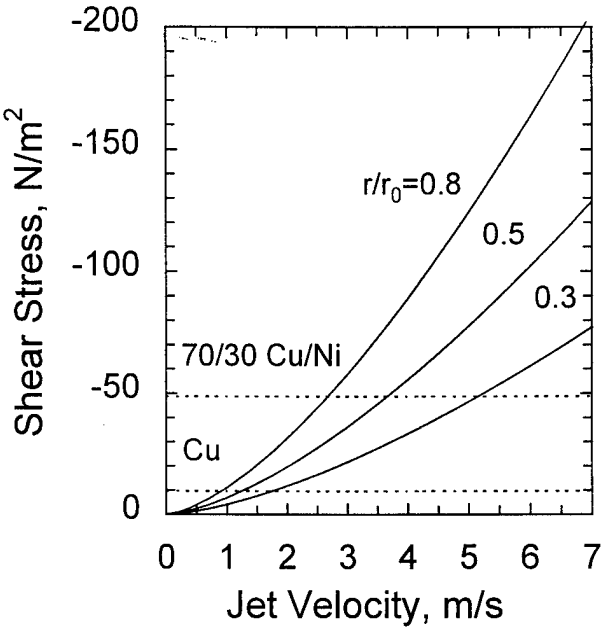

Figure 1. Shear stress as a function of jet velocity with dimensionless radial position on the electrode surface as a parameter for the impinging jet cell used in the present work. Critical shear stress values reported by Efird[6] are presented for reference.

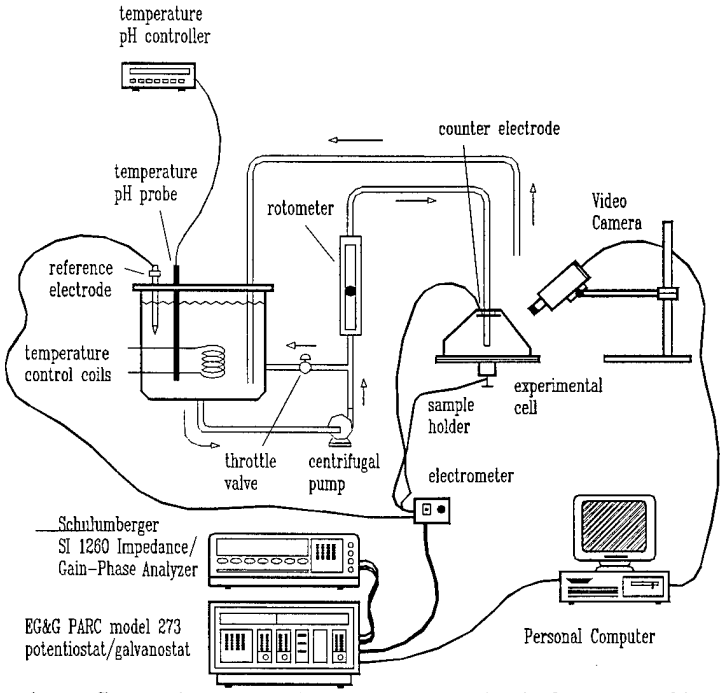

Figure 2. Experimental configuration used for measuring the influence of jet velocity on the corrosion of copper and copper alloys in synthetic seawater.

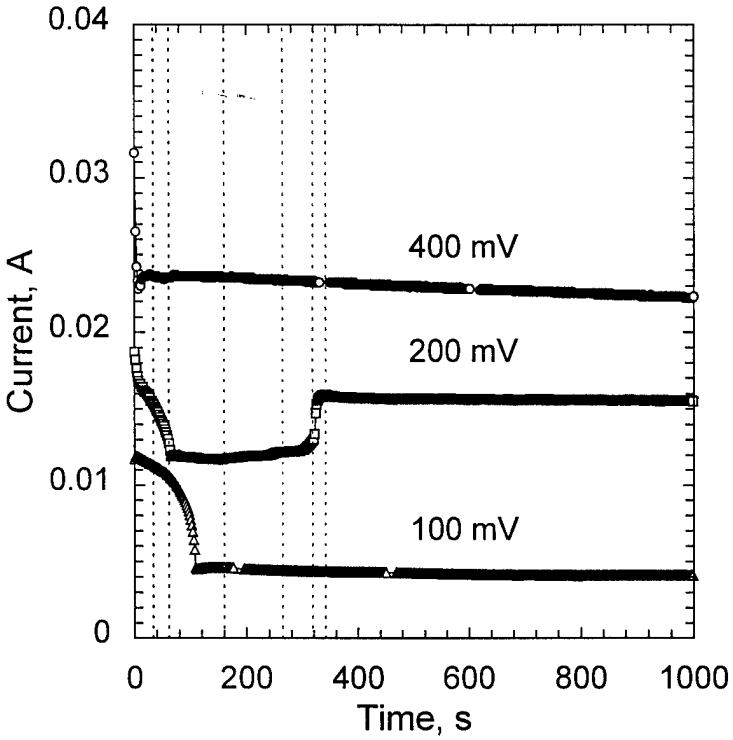

Figure 3. Current as a function of time for 99.9% copper in aerated synthetic seawater at a jet velocity of 0.1 m/s. The dashed lines correspond to the time at which images shown in Figure 4 were collected for the coupon held at 200 mV (SCE).

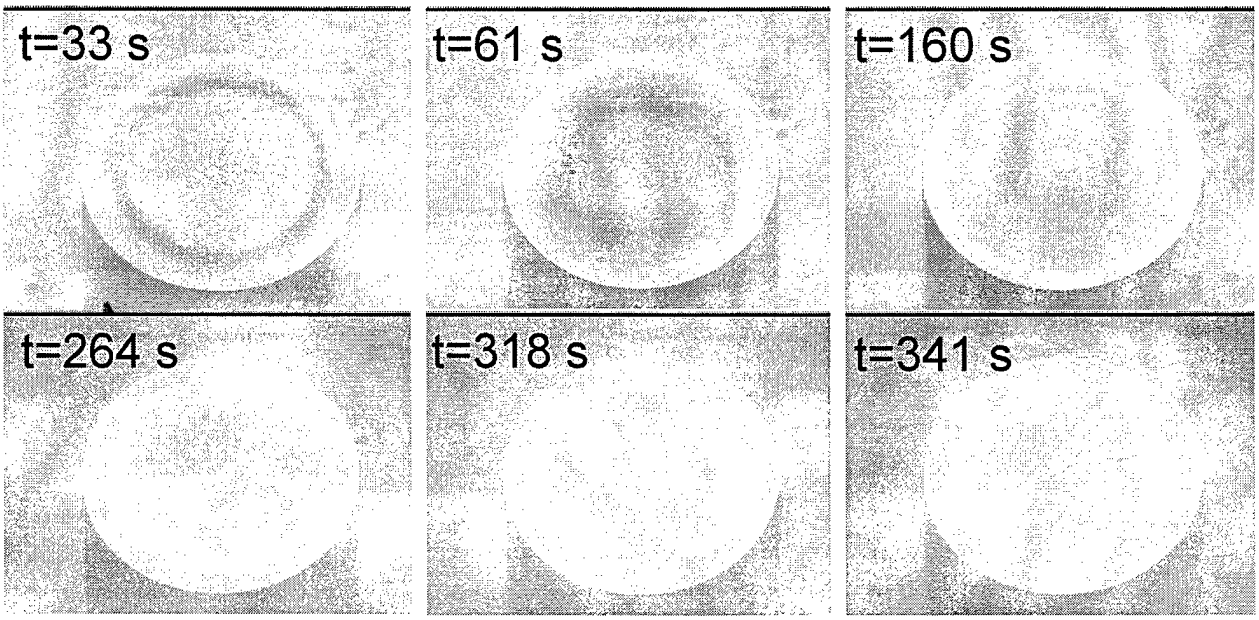

Figure 4 Video images collected for the coupon held at 200 mV(SCE) in Figure 3.

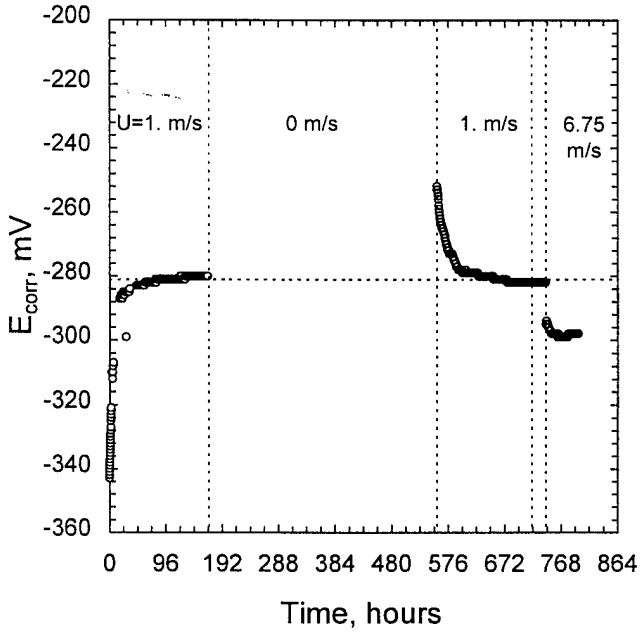

Figure 5. Corrosion potential as a function of time for 99.9% Cu in passively-aerated synthetic seawater. The time period for the experiment was 33 days. The electrode remained in stagnant fluid from t=190 to 550 hours, a cathodic potential was applied at t=556 hours, and flow was resumed at t=557 hours.

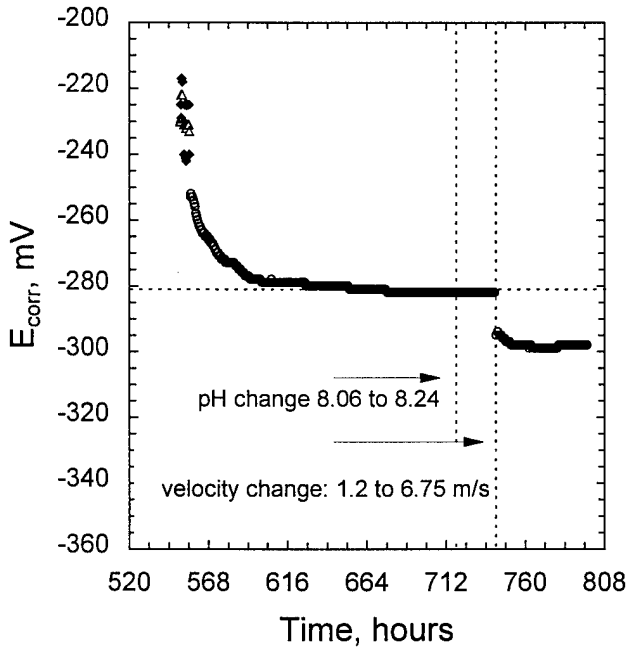

Figure 6. Corrosion potential as a function of time for the latter stage of the experiment presented in Figure 5.

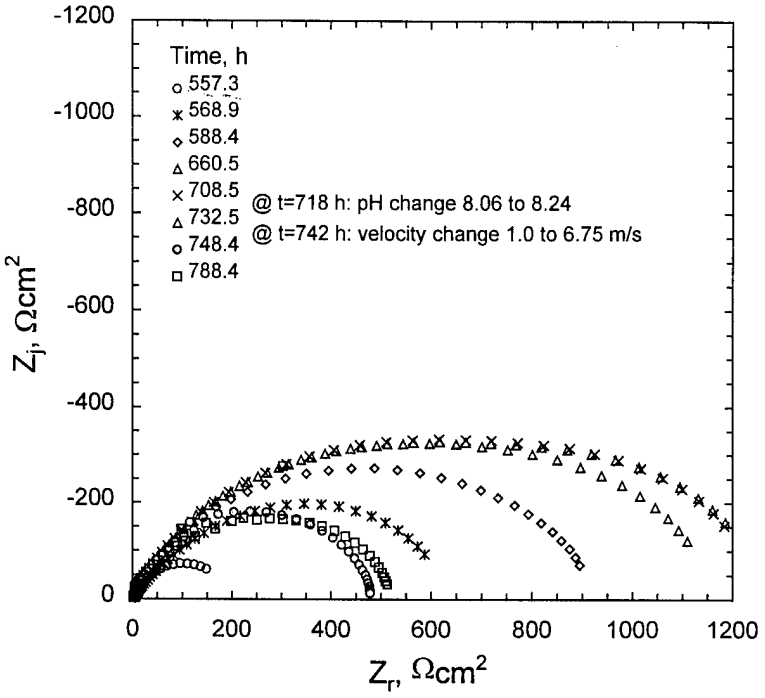

Figure 7. Impedance data collected for over the course of 231 hours corresponding to the corrosion potential data in Figure 6.

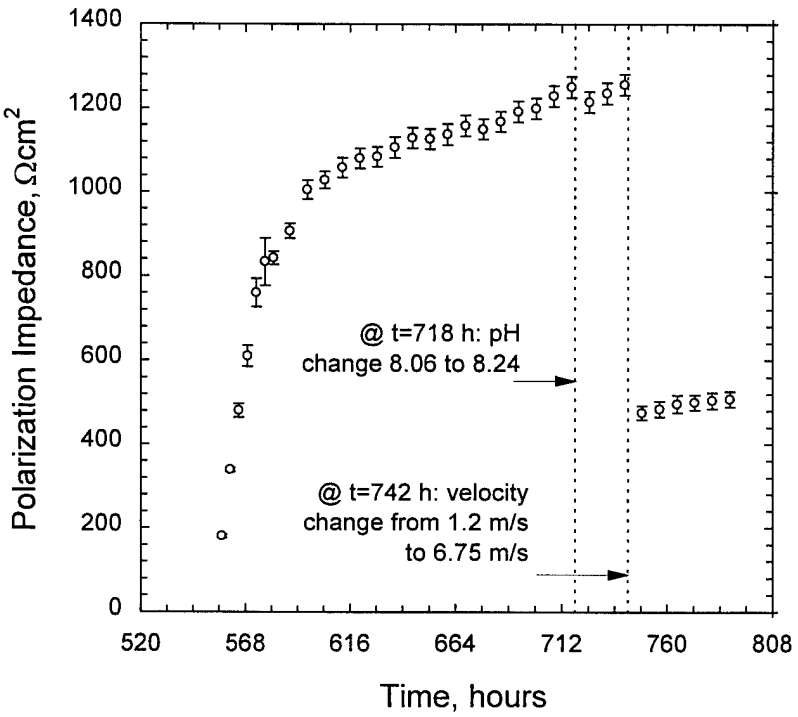

Figure 8. Polarization impedance for the impedance scans shown in Figure 7. Estimated values and associated standard deviation were obtained through the use of a measurement model.

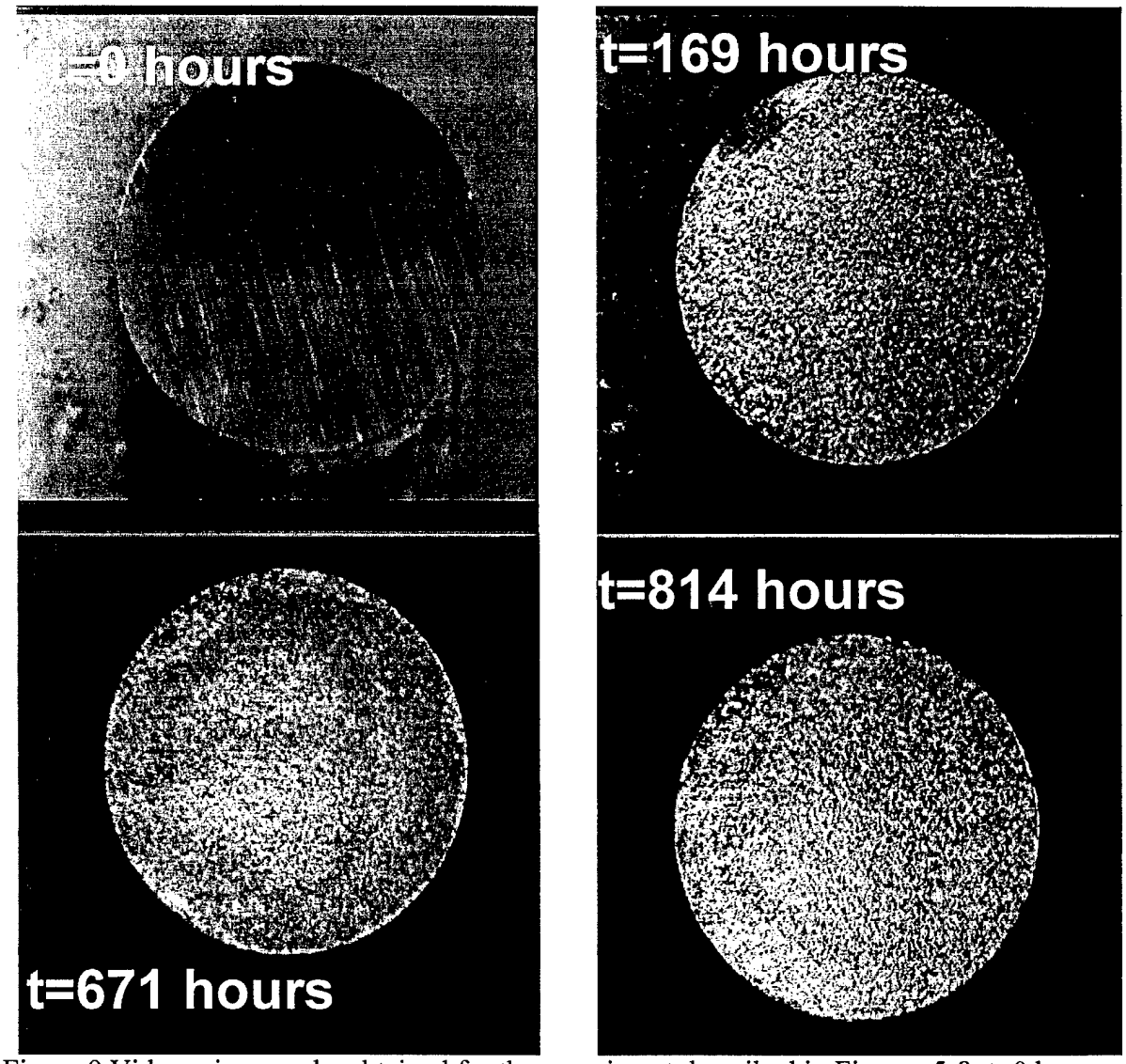

Figure 9 Video micrographs obtained for the experiment described in Figures 5-8; t=0 hours: the initial condition immediately after submersion; t=169 hours: after steady flow at 1 m/s; t=671 hours: before increase in jet velocity; and t=814 hours: after increase in jet velocity.

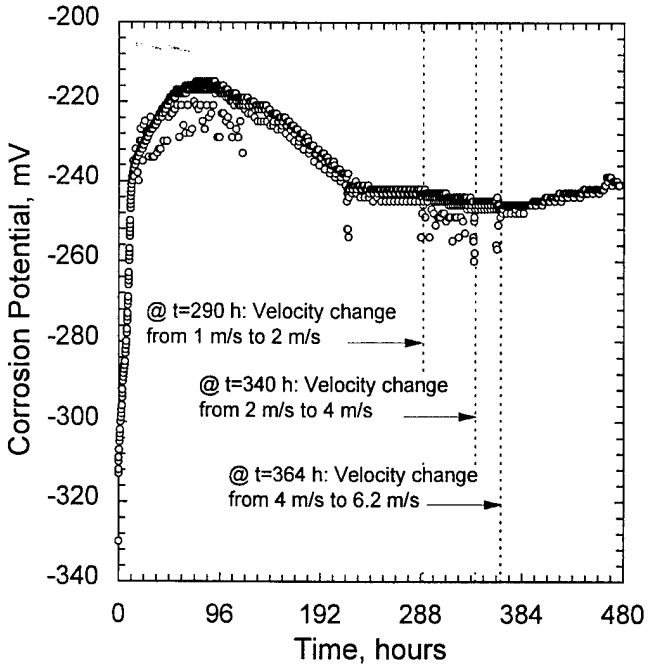

Figure 10. Corrosion potential as a function of time for 99.9% copper in continuously aerated synthetic seawater electrolyte.

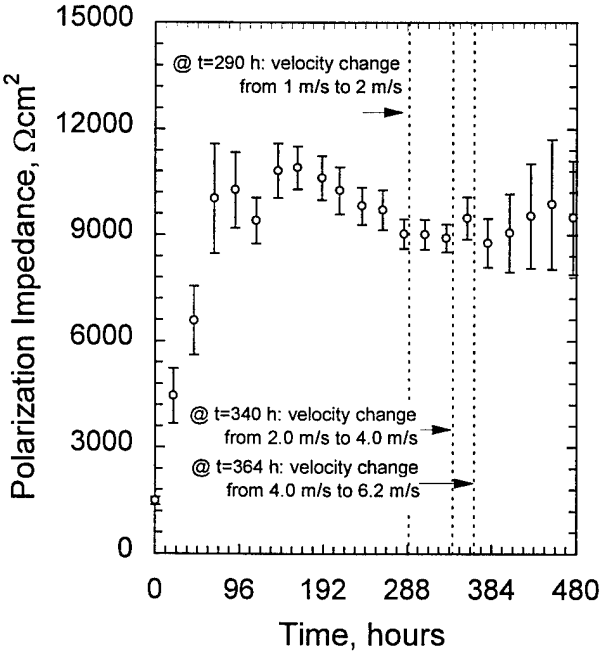

Figure 11. Polarization impedance for the impedance data collected during the experiment shown in Figure 10. Estimated values and associated standard deviation were obtained using a measurement model.